coatings

MDPI

Article

Effect of Strain Levels on the Corrosion Resistance of an Enamel-Coated Steel Rebar

Fujian Tang [1,*], Hao Cui [1], Gang Li [1] and Shangtong Yang [2]

[1] School of Civil Engineering, Dalian University of Technology, Dalian 116024, China
[2] Department of Civil and Environmental Engineering, University of Strathclyde, Glasgow G1 1XQ, UK
* Correspondence: ftang@dlut.edu.cn

Abstract: The effect of strain levels on the corrosion resistance of an enamel-coated steel rebar is experimentally investigated in this study. Enamel coating was applied on the surface of a steel rebar by using the wet process. A strain gauge was attached on the surface of the coated steel rebar to record the strain levels and a plastic container was mounted for electrochemical corrosion tests. A stress-corrosion test set-up was designed to conduct corrosion and tensile tests simultaneously. The strain levels considered include 0 με, 300 με, 600 με, 900 με and 1200 με, and the electrochemical techniques employed include open circuit potential, linear polarization resistance and electrochemical impedance spectroscopy. The microstructure of the enamel coating was also examined with scanning electron microscopy. Results show that the enamel coating has a thickness of ~150 μm, and there are some air bubbles in the coating. The average corrosion current density of the uncoated steel rebar decreases from 18.64 μA/cm^2 to 14.39 μA/cm^2 in NaCl solution due to the generation of corrosion products. The corrosion current density of the enamel-coated steel rebar gradually increases from 0.49 μA/cm^2 when the strain is zero to 0.65 μA/cm^2 as strain reaches 1200 με, which is almost 40 times lower than that of the uncoated steel rebar. Impedance spectrum results show that the corrosion resistance of enamel coating decreases with an increase in the tensile strain level; however, it still protects steel rebar from corrosion to some degree.

Keywords: steel rebar corrosion; enamel coating; stress level; electrochemical impedance spectroscopy; linear polarization resistance

Citation: Tang, F.; Cui, H.; Li, G.; Yang, S. Effect of Strain Levels on the Corrosion Resistance of an Enamel-Coated Steel Rebar. *Coatings* **2023**, *13*, 510. https://doi.org/10.3390/coatings13030510

Academic Editor: Edoardo Proverbio

Received: 24 December 2022
Revised: 21 February 2023
Accepted: 23 February 2023
Published: 25 February 2023

1. Introduction

The surface of steel rebars in reinforced concrete (RC) structures is initially covered with a protective passive film, which is formed due to the alkaline environment of the fresh concrete. However, with an increase of service life, this protective film gradually loses its function and corrosion occurs in the steel rebar due to carbonization of the concrete cover or diffusion of chloride from the environment [1–3]. Corrosion reduces the cross-sectional area and the mechanical properties of steel rebar [4], causes cracking, delamination and spalling of the concrete cover [5,6], leads to bond strength loss between the steel rebar and concrete [7], and finally results in a reduction in the carrying capacity and service life of RC structures [8,9].

Over the past decades, various methods have been developed to protect steel rebar in the RC structure from corrosion attack. One of the most effective and efficient methods is the use of a protective coating on the surface of steel rebar, as it can establish a physical barrier between the aggressive environment and the steel rebar under protection. Fusion bonded epoxy coating is one of the most widely used coatings for steel rebar. However, it reduces the bond strength with concrete and is prone to under-film corrosion if damaged during transportation or handling [10,11]. Hot-dip galvanized coating is also used in RC structures. However, chemical reactions might occur between the zinc coating and the concrete, especially in the curing stages of the concrete, and these chemical reactions

produce hydrogen gas and increase the porosity of the interface between the galvanized steel rebar and the concrete, and consequently reduce the bond strength [12].

Vitreous enamel, an inorganic coating, is made by firing powdered glass onto the surface of a metal substrate at temperature between 750 °C and 850 °C. The oxides in the enamel powder would react with the element in the steel, such as carbon, to form a chemical bond between the enamel coating and the steel substrate, which prevents potential under-film corrosion [13]. Due to its glassy nature, the enamel coating has a shining and smooth surface, and is, thus, widely used for household and industrial applications. Moreover, enamel coating also demonstrates many advantages, such as a high resistance to abrasion, resistance to chemicals (i.e., both acidic and alkaline solutions), resistance to fire and high temperature and resistance to detergents [14]. Furthermore, its properties are flexible and can be adjusted by modifying the chemical composition of the frits [15]. For example, the corrosion resistance to alkaline solution shows a significant increase by adding zirconia, lithium oxides and milling additives based on quartz [16]; the resistance to acid can be enhanced by adding quartz and zirconium oxide [17]; the adhesion with substrate metal could be improved by adding NiO or CoO [18]; and crystallization treatment can improve the hardness of the enamel coating [19].

By adding cement powder or calcium silicate in the enamel frit, chemically reactive enamel coatings have been proposed for enhanced corrosion resistance and improved bond strength of steel reinforcement in concrete structures in the past decade. The microstructure, phase composition and corrosion resistance of enamel coating applied on smooth steel bars have been experimentally investigated, and results show that although the interconnected regions of calcium silicate particles provide a pathway for the penetration of aggressive chemicals, the chemically reactive enamel coating increases the corrosion resistance of steel rebars to some extent [20]. The long-term corrosion mechanism and rate of chemically reactive enamel coating applied on smooth steel bars embedded in mortar was also studied [21]. Different from smooth steel bar, deformed steel bars are widely used in reinforced concrete structures. However, the thickness of enamel coating is not uniformly distributed due to the presence of rebar deformation. Moreover, there is also some damage during transportation and handling at the construction site. Therefore, the short-term and long-term corrosion performance of chemically reactive enamel coating applied to a deformed steel rebar have also been studied; the effect of impact damage was considered and the performance was compared with fusion bonded epoxy coating [13,22]. In addition, the chloride threshold and adhesion strength with substate steel have also been investigated by pull-off tests, and results show that the addition of cement increased the adhesion strength with steel compared with pure enamel, and the chloride threshold of enamel-coated steel is greater than that of uncoated steel [23]. Regarding the bond strength with concrete, the presence of chemically reactive enamel coating reduces the porosity of the interfacial transition zone between steel and concrete, and results in an increase in the bond strength with concrete [24,25]. The microstructure and properties are dependent on the parameter of the enameling process, and, therefore, the effect of sintering temperature and coating cycles on the microstructure, phase composition and corrosion resistance have also been experimentally investigated [26–28].

In practical engineering applications, the enamel-coated steel rebar is in a state of tension or compression to resist the loadings imposed on the structures. For compression members, such as reinforced concrete columns, enamel coating is in compression and the corrosion resistance may not be an issue. However, for reinforced concrete members in bending or tension, the enamel-coated steel rebar is in a state of tension. As mentioned previously, enamel coating has a glassy nature and is brittle; therefore, some micro-cracks generated in the coating are possible if it is subjected to a larger deformation. However, the effect of tensile stress levels on the corrosion resistance of enamel-coated steel rebar has not been investigated and fully understood.

Therefore, this study aims to experimentally investigate the effect of tensile strain levels on the corrosion resistance of an enamel-coated steel rebar. A stress-corrosion test

set-up was designed to conduct both electrochemical corrosion tests and tensile tests simultaneously. The enamel-coated steel rebar was first tensioned to different strain levels and then electrochemical corrosion tests, including open circuit potential, linear polarization resistance and electrochemical impedance spectroscopy, were conducted. For comparison, an uncoated steel rebar was also prepared and tested.

2. Materials and Methods

2.1. Preparation of the Enamel-Coated Steel Rebar

A HRB400 steel rebar with a dimeter of 12 mm was used in this study, and its chemical composition is shown in Table 1. The steel rebar was cut into ~300 mm long pieces, and the two ends were screw threaded for applying tensile strain during the corrosion tests. After the screw thread processing, the steel rebars were cleaned with a sand blaster and rinsed with acetone before enamel coating.

Table 1. Chemical composition of the steel rebar used in this study.

Elements	C	Si	Mn	P	S	Cr	Ni	Cu	Mo	V	Fe
wt.%	0.240	0.390	1.260	0.023	0.027	0.180	0.040	0.090	0.002	0.002	97.746

Commercially available enamel powder was used, and its chemical composition is shown in Table 2. The enamel powder was mixed with tap water with a weight ratio of 1.0:2.35 to form the enamel slurry. The cleaned steel rebars were dipped in the enamel slurry until the entire surface was fully covered with wet enamel. The wet enamel-coated steel rebars were moved into a furnace with a temperature of 60 °C for 10 min to remove moisture. During the preheating process, the enamel-coated steel rebars were rotated constantly to ensure a uniform enamel coating layer on the steel rebars. After the preheating process, the temperature of the furnace was gradually increased up to 840 °C and fired for 10 min. After 10 min, the temperature of the furnace decreased gradually to room temperature and, finally, the enamel-coated steel rebars were produced.

Table 2. Chemical composition of the enamel powder used in this study.

Oxides	SiO_2	Al_2O_3	B_2O_3	$NaNO_3$	CaF	KCO_3	Li_2CO_3	TiO_2	CoO	NiO	MnO_2	$NaCO_3$
wt.%	37.8	15.8	14.6	4.8	3.6	6.7	5.4	2.7	0.5	1.2	5.2	1.7

To control the strain levels during the stress-corrosion tests, a strain gauge was attached on the surface of the enamel-coated steel rebars, as shown in Figure 1a. In addition, a plastic container made of polyethylene terephthalate (PET, molecular formula $(C_{10}H_8O_4)_n$) was mounted with the steel rebar for electrochemical corrosion tests. A round hole was drilled in the bottom of the plastic container and the steel rebar passed through the hole, then epoxy resin was applied to seal the gap between the steel rebar and the plastic container. Although a small amount (~6 ng/L) of antimony (Sb) would migrate from the PET to the solution [29], its effect on the corrosion reaction of steel is insignificant. Moreover, it is easier to drill a hole in the bottom of a plastic container and fix it with the steel rebar compared to the glass container. The steel rebars mounted with a plastic container and ready for tests are shown in Figure 1b. To ensure the repeatability of the test results, three enamel (PE)-coated steel rebars and three uncoated (UN) steel rebars were prepared and tested.

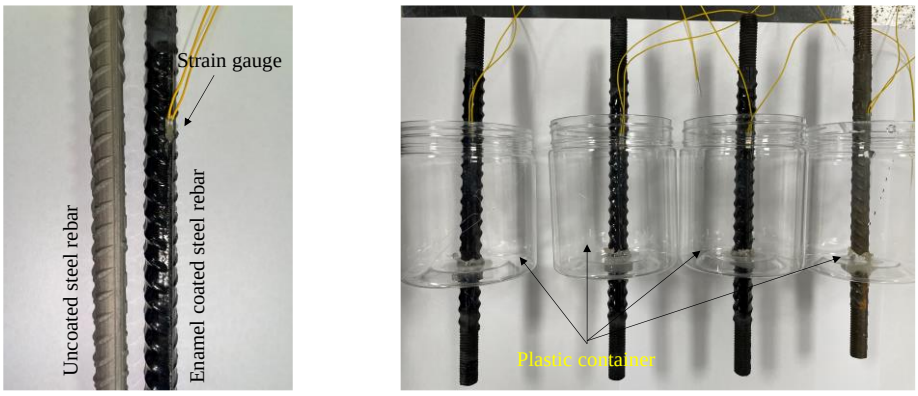

(**a**) (**b**)

Figure 1. (**a**) Uncoated and enamel-coated steel rebar; (**b**) three enamel steel rebars and one uncoated steel rebar mounted with a plastic container.

2.2. Stress-Corrosion Test Set-Up

Figure 2 shows the stress-corrosion test set-up. The two screwed ends of the steel rebar were fixed with two 20 mm thick steel plates by using screws. A hydraulic jack was placed between the two steel plates to apply force against the top plate. Regarding the corrosion test, the plastic container was filled with 3.5 wt.% NaCl solution which was made by mixing purified sodium chloride powder in de-ionized water. The loading was first applied to a designated strain level which was controlled by the strain gauge reading, and then electrochemical corrosion tests were conducted. The strain levels investigated in this study included 0 με, 300 με, 600 με, 900 με and 1200 με. The electrochemical corrosion techniques employed include open circuit potential, linear polarization resistance and electrochemical impedance spectroscopy (EIS). A three-electrode system was applied including the steel rebar as the working electrode, a platinum sheet with 20 mm × 20 mm × 0.2 mm as the counter electrode and a saturated calomel electrode (SCE) as the reference electrode, as shown in Figure 2. Linear polarization resistance was conducted by applying a potential from −20 mV to 20 mV around the open circuit potential with a scan rate of 0.167 mV/s. EIS tests were conducted by applying a sinusoidal potential of 10 mV around the open circuit potential with frequency ranging from 100 kHz to 5 mHz with 5 points per decade of frequency.

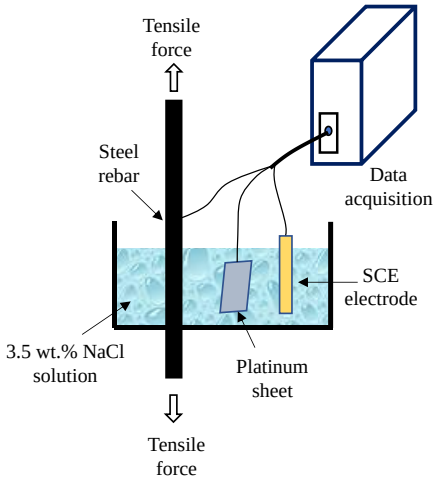

Figure 2. Schematic illustration of the stress-corrosion test set-up.

2.3. Microstructural Observation

To investigate the microstructure of the enamel coating, an additional enamel-coated steel rebar was fabricated in the laboratory. The enamel-coated steel rebar was first placed in a PVC pipe with an inside diameter of 20 mm and then filled with epoxy resin. After curing for 24 h, a ~50 mm long piece was cut with a band saw and sectioned in the middle into two halves with a machine. The cross-sections were polished successively with silicate carbide papers of grade 60, 180, 320, 480, 600, 800 and 1200, then rinsed with de-ionized water and acetone, and dried in an oven prior to microstructural observation with scanning electron microscopy (Hitachi SU5000, Tokyo, Japan).

3. Results and Discussion

3.1. Microstructure of the Enamel Coating

Figure 3 shows the cross-sectional SEM microstructure of the enamel coating investigated in this study. It has a thickness of approximately 150 μm and contains some air bubbles near the interface with the steel rebar. The presence of air bubbles is attributed to the chemical reactions between oxides and water in the enamel and carbon in the steel rebar at firing temperatures that that release carbon dioxide and hydrogen gases [23].

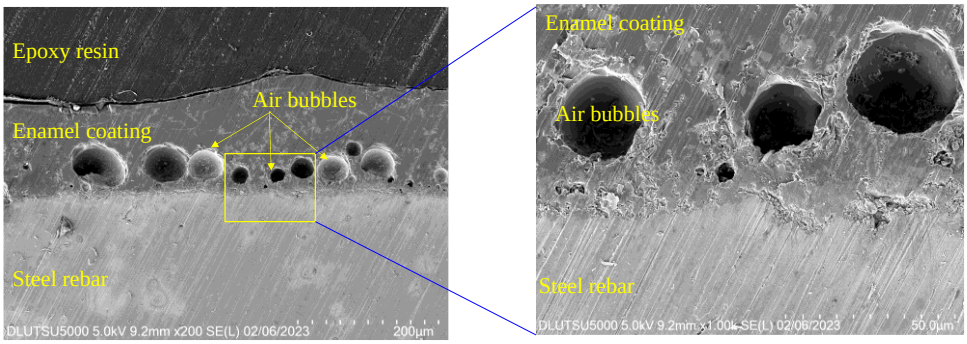

Figure 3. Microstructure of enamel coating.

3.2. OCP and Linear Polarization Resistance

The open circuit potential (OCP) of uncoated and three enamel-coated steel rebars immersed in 3.5 wt.% NaCl solution is shown in Figure 4. Each point represents the average of three specimens with an error bar representing one standard deviation. The average OCP of the uncoated steel rebar is around −625 mV/SCE when the tensile strain is zero, then decreases to be around −690 mV/SCE when the tensile strain increases to 300 με, and then remains stable as the tensile strain increases up to 1200 με. Regarding the enamel-coated steel rebars, the average OCP is around −660 mV/SCE, and the tensile strain level does not affect the OCP significantly.

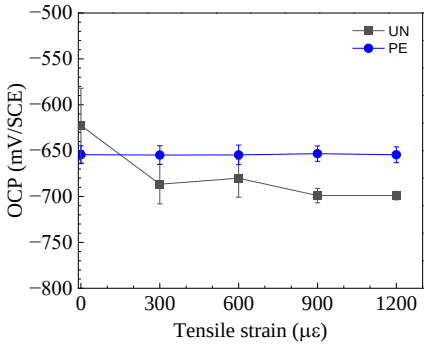

Figure 4. Open circuit potential of uncoated (UN) and enamel (PE)-coated steel rebars at different strain levels in 3.5 wt.% NaCl solution.

Figure 5a compares the polarization resistance of uncoated steel rebar with that of the enamel-coated steel rebar at different strain levels, which was obtained from the linear polarization resistance curve. The average polarization resistance of three uncoated steel rebars is 1.51 kΩ cm^2 when the tensile strain is zero, and it increases to 1.76 kΩ cm^2 when the tensile strain in the streel rebar reaches 300 με. With an increase in the tensile strain level, the polarization resistance gradually increases and finally reaches 1.85 kΩ cm^2 when the tensile strain in the streel rebar is 1200 με. The increase in the polarization resistance with an increase in strain levels is mainly attributed to the generation of corrosion products that accumulated on the steel rebar surface and slowed down the diffusion of oxygen. The average polarization resistance of the enamel-coated steel rebar is 54.43 kΩ cm^2 when the tensile strain is 0 με, and it decreases to 45.07 kΩ cm^2 when the tensile strain reaches 300 με, as shown in Figure 5a. With a further increase in the tensile strain, the polarization resistance continues to decrease and reaches 42.07 kΩ cm^2 when the tensile strain is 1200 με. The decrease in the polarization resistance with the increase in tensile strain level is mainly attributed to the micro-cracks generated in the enamel coating due to tensile stress in the steel rebar.

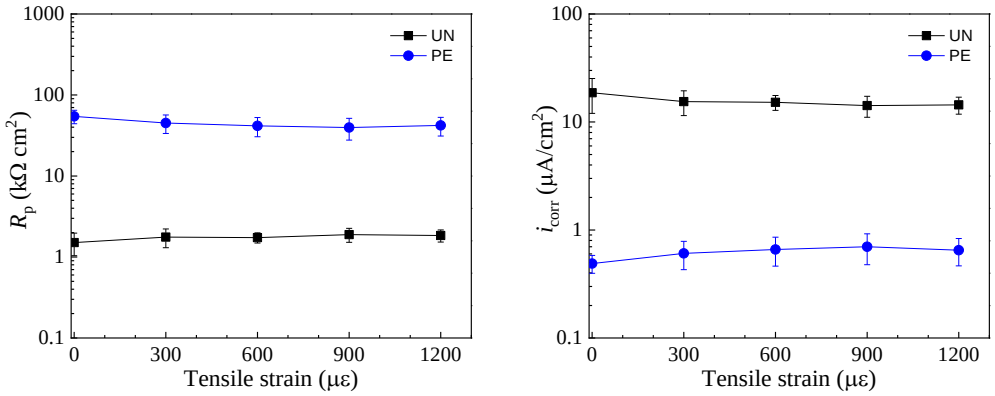

Figure 5. (**a**) Polarization resistance and (**b**) corrosion current density of the uncoated (UN) and enamel (PE)-coated steel rebar in 3.5 wt.% NaCl solution at different strain levels.

The corrosion current density of both uncoated and enamel-coated steel rebars at different tensile strain levels was calculated by using the following equation [21]:

$$i_{corr} = \frac{B}{R_p} \quad (1)$$

where R_p is the polarization resistance obtained from the linear polarization curve and B is the constant associated with the Tafel slopes; B = 26 mV was used in this study [23]. Figure 5b compares the average corrosion current density of uncoated and enamel-coated steel rebars. The corrosion current density of the uncoated steel rebar in 3.5 wt.% NaCl solution is 18.64 μA/cm^2 when the tensile strain is 0 με, and decreases to 15.45 μA/cm^2 and 14.39 μA/cm^2 when the tensile strain is 300 με and 1200 με, respectively. For enamel-coated steel rebars, the average corrosion current density is around 0.49 μA/cm^2 when the tensile strain is 0 με. The corrosion current density increases with an increase in the tensile strain in the enamel-coated steel rebar, and reaches 0.65 μA/cm^2 when the tensile strain is 1200 με. Although the corrosion resistance of the enamel-coated steel rebar decreases with an increase in the tensile strain, the enamel coating still provides the steel rebar with significant protection from corrosion.

3.3. EIS

Figure 6 shows the impedance spectrum of a representative uncoated steel rebar in 3.5.wt.% NaCl solution at different tensile strain levels in the format of both Nyquist and Bode plots. Depressed semi-circles are observed in the Nyquist plots, as shown in Figure 6a, and the radius of the semi-circle is approximately 750 Ωcm^2, as there is no tensile strain in the uncoated steel rebar. The radius of the semi-circle gradually increases with an increase in the tensile strain levels. One time constant is present in the Bode plots, as shown in Figure 6b, corresponding to the interfacial properties between the solution and the rebar steel, i.e., the double layer. The scatter symbols represent measured data, while the continuous line represents the results fitted by using the equivalent electrical circuit, as shown in Figure 7a. In Figure 7a, R_s is the solution resistance, R_{ct} is the charge transfer resistance and CPE_{dl} represents the non-ideal capacitive behavior of the double layer between the solution and the rebar steel where corrosion occurred. CPE is the abbreviation of the constant phase element, which is used to consider the non-homogeneity of the electrochemical system that mainly arises from irregularities on the steel surface, the surface roughness, fractal surface and irregular distribution of the applied potential [13]. The CPE can be mathematically expressed as [30]

$$Y_{CPE} = Y(j\omega)^n \quad (2)$$

where Y is the parameter with units of $\Omega^{-1}cm^{-2}sn$, ω is the angular frequency in rad/s and n reflects the deviated degree of the capacitance of the electrode from the ideal capacitor. The CPE is a capacitor when $n = 1$, a resistor when $n = 0$, an inductor when $n = -1$ and Warburg diffusion impedance when $n = 0.5$.

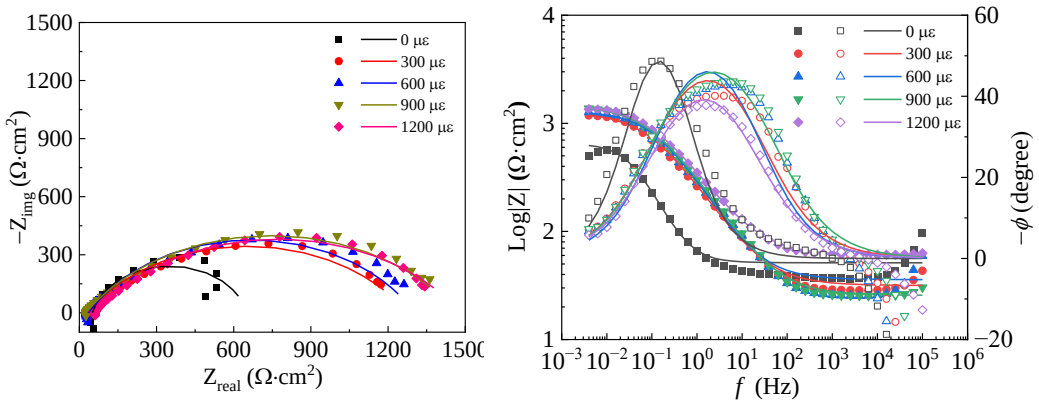

Figure 6. Impedance spectrum of a representative uncoated steel rebar immersed in 3.5 wt.% NaCl solution at different strain levels: (**a**) Nyqusit plots and (**b**) Bode plots.

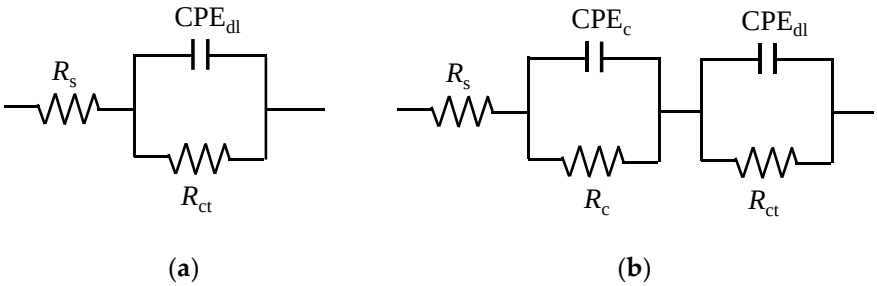

Figure 7. Equivalent electrical circuit: (**a**) uncoated steel rebar and (**b**) enamel-coated steel rebar.

The impedance spectra of a representative enamel-coated steel rebar in 3.5 wt.% NaCl solution at different tensile strain levels are shown in Figure 8. As shown in Figure 8a, the magnitude of the impedance of the enamel-coated steel rebar is almost 60 times greater than that of the uncoated steel rebar. Different from that of the uncoated steel rebar (see Figure 6), two depressed semi-circles are observed for the enamel-coated steel rebar in the Nyquist plots, as displayed in Figure 8a, and, accordingly, two time-constants are present in the Bode plots, as shown in Figure 8b. The time-constant in the high frequency range is attributed to the properties of the enamel coating, while the time-constant in the low frequency range is associated with the double layer at the interface between the solution and the rebar steel. The equivalent electrical circuit used to fit the impedance spectrum of the enamel-coated steel rebar is shown in Figure 7b. In addition to the two parameters related to the double layer, two additional parameters associated with the enamel coating are introduced, in which CPEc represents the non-ideal capacitive behavior of the enamel coating and R_c is the enamel coating resistance. The fitted results are the continuous lines in Figure 8, indicating satisfactory fitting.

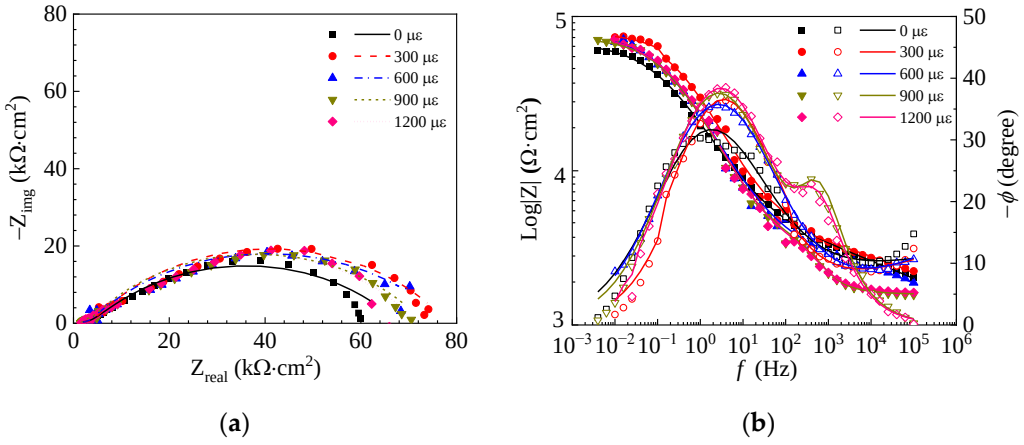

Figure 8. Impedance spectra of a representative enamel-coated steel rebar at different strain levels in the format of (**a**) Nyquist plots and (**b**) Bode plots.

Figure 9 shows the effect of tensile strain on the average enamel coating resistance, which was extracted from the fitted results of the equivalent electrical circuit. It can be observed that the average enamel coating resistance decreases from 10.44 kΩ cm^2 to 1.50 kΩ cm^2 as the tensile strain increases from 0 με to 1200 με. The dramatic decrease in the enamel coating resistance is attributed to the generation of micro-cracks in the enamel coating under tensile strain. The micro-crack provides a pathway for the solution to penetrate through and reach the steel rebar, and, consequently, the coating resistance decreases.

The charge transfer resistance of both the uncoated and the enamel-coated steel rebar specimens in 3.5 wt.% NaCl solution at different tensile strain levels is compared and shown in Figure 10. Once immersed in the solution, the average charge transfer resistance of the uncoated steel rebar is 1.21 kΩ cm^2 and it increases gradually up 1.72 kΩ cm^2 as the tensile strain of the steel rebar increases to 1200 με. For the enamel-coated steel rebar, the average charge transfer resistance increases from 55.05 kΩ cm^2 to 66.04 kΩ cm^2 as the tensile strain increases from 0 με to 600 με, and then gradually decreases to 57.42 kΩ cm^2 as the tensile strain reaches 1200 με. Despite of the variation of the charge transfer resistance of the enamel-coated steel rebar specimens, the R_{ct} of the enamel-coated steel rebar is still around 40 times greater than that of the uncoated steel rebar. Therefore, enamel coating still provides the steel rebar with strong protection against corrosion even when subjected to tensile strain, which is consistent with the results of polarization resistance, as shown in Figure 5a.

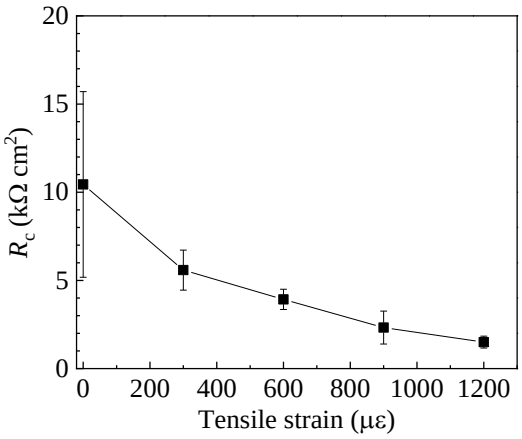

Figure 9. Effect of the tensile strain level on the enamel coating resistance.

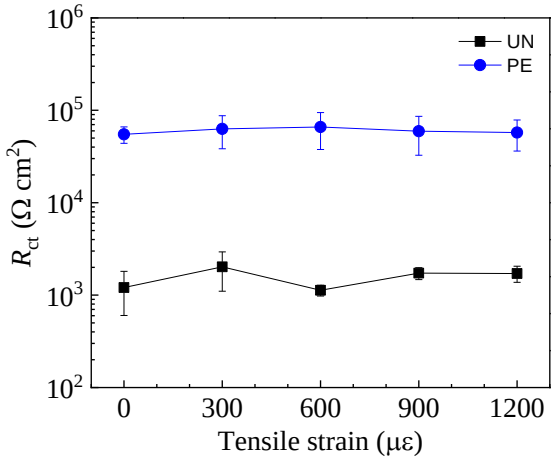

Figure 10. Comparison of the charge transfer resistance of the uncoated (UN) and enamel (PE)-coated steel rebar.

It is noted that the open circuit potential (OCP) of the enamel-coated steel rebar is close to that of the enamel-coated steel rebar, as shown in Figure 4, while a significant difference is observed regarding the polarization resistance (see Figure 5) and the impedance parameters (see Figure 10). This is because the OCP indicates the corrosion state of the steel rebars, while both the polarization resistance and the electrochemical impedance reflect the rate of corrosion, i.e., the rate of electron transfer between the steel rebar and the NaCl solution [17]. The close OCP between uncoated and enamel-coated steel rebars indicates that both are in a state of active corrosion; however, the corrosion rate of the enamel-coated steel rebar is significantly lower than that of the uncoated steel rebar, based on both polarization resistance and impedance results. In addition, the linear polarization resistance is comparable with electrochemical impedance spectroscopy, and both demonstrate the same degree of improvement in the corrosion resistance for the steel rebar after enamel coating.

In previous studies, the corrosion resistance of enamel coating was also investigated by coating on both smooth [20] and deformed steel rebars [13]. The results showed that the coating resistance of enamel, when applied on a smooth steel rebar, was 8.6 kΩ cm^2 [20], while it was 1.3 kΩ cm^2 when applied on a deformed steel rebar [20]. In this study, the coating resistance of enamel is 10.44 kΩ cm^2 when the tensile strain is 0 με, which is significantly higher than that in previous studies. This is mainly attributed to the different microstructure of the two enamel coatings. Many air bubbles were present and uniformly distributed in the enamel coating used in previous studies [13,20], while less air bubbles were observed and only concentrated near the interface with the rebar steel for the enamel coating used in this study, as shown in Figure 3. In addition, the coating resistance of

low-temperature sintered enamel coatings was around 30.00 kΩ cm^2 [26], which is almost three times higher than that used in this study. This is because the thickness of the low temperature sintered enamel coating was around 300 μm, which is twice the thickness of the enamel coating investigated in this study.

4. Conclusions

The effect of tensile strain levels on the corrosion resistance of enamel-coated steel rebar in 3.5 wt.% NaCl solution was experimentally investigated in this study. The electrochemical techniques used include open circuit potential, linear polarization resistance and electrochemical impedance spectroscopy. The tensile strain levels investigated were 0 με, 300 με, 600 με, 900 με and 1200 με. The microstructure of the enamel coating was also examined. Based on the results and discussion, the following conclusions can be drawn:

(1) The enamel coating has a thickness of ~150 μm, and there are some air bubbles in the coating which are formed due to the release of carbon dioxide and hydrogen gases from chemical reactions between enamel oxides and carbon element in the steel rebar during the firing process.

(2) The corrosion current density of the uncoated steel rebar decreases from 18.64 μA/cm^2 to 14.39 μA/cm^2 in NaCl solution due to the generation of corrosion products. The average corrosion current density of the enamel-coated steel rebar is 0.49 μA/cm^2, which is around 40 times lower than that of the uncoated steel rebar. The corrosion current density of the enamel-coated steel rebar increases with an increase in the tensile strain level, and it reaches 0.65 μA/cm^2 when the tensile strain is 1200 με. The decrease in the corrosion resistance is attributed to the micro-cracks generated in the enamel coating under the tensile strain.

(3) The tensile strain reduces the enamel coating resistance, and it decreases from 10.44 kΩ cm^2 to 1.50 kΩ cm^2 as the tensile strain increases from 0 to 1200 με. The charge transfer resistance of the enamel-coated steel rebar remains around 40 times greater than that of the uncoated steel rebar when the tensile strain is 1200 με. Therefore, enamel coating still provides steel rebar with strong protection against corrosion subjected even to tensile strain.

Author Contributions: Conceptualization, F.T.; methodology, F.T. and H.C.; software, H.C.; validation, F.T., H.C. and S.Y.; formal analysis, H.C. and S.Y.; investigation, H.C.; data curation, H.C.; writing—original draft preparation, F.T.; writing—review and editing, G.L. and S.Y.; visualization, S.Y.; supervision, F.T. and G.L.; project administration, G.L.; funding acquisition, F.T. and G.L. All authors have read and agreed to the published version of the manuscript.

Funding: This study was supported by the National Natural Science Foundation of China (No. 52078099 and 52225804).

Institutional Review Board Statement: Not applicable.

Informed Consent Statement: Not applicable.

Data Availability Statement: Some or all data that support the findings of this study are available from the corresponding author upon reasonable request.

Conflicts of Interest: The authors declare no conflict of interest.

References

1. Angst, U.M. Challenges and opportunities in corrosion of steel in concrete. *Mater. Struct.* **2018**, *51*, 4. [CrossRef]
2. Andrade, C. Propagation of reinforcement corrosion: Principles, testing and modelling. *Mater. Struct.* **2019**, *52*, 2. [CrossRef]
3. Andrade, C.; Izquierdo, D. Statistical treatments of chloride threshold and corrosion propagation rate. *Corros. Mater. Degrad.* **2022**, *3*, 598–611. [CrossRef]
4. Tang, F.; Lin, Z.; Chen, G.; Yi, W. Three-dimensional corrosion pit measurement and statistical mechanical degradation analysis of deformed steel bars subjected to accelerated corrosion. *Constr. Build. Mater.* **2014**, *70*, 104–117. [CrossRef]
5. Li, C.; Yang, S. Prediction of concrete crack width under combined reinforcement corrosion and applied load. *ASCE J. Eng. Mech.* **2011**, *137*, 722–731. [CrossRef]

6. Andrade, C.; Cesetti, A.; Mancini, G.; Tondolo, F. Estimating corrosion attack in reinforced concrete by means of crack opening. *Struct. Concr.* **2016**, *17*, 533–540. [CrossRef]
7. Tang, F.; Lin, Z.; Qu, H.; Chen, G. Investigation into corrosion-induced bond degradation between concrete and steel rebar with acoustic emission and 3D laser scan techniques. *J. Infrastruct. Preserv. Resil.* **2022**, *3*, 5. [CrossRef]
8. Zhang, W.; Zhang, H.; Gu, X.; Liu, W. Structural behavior of corroded reinforced concrete beams under sustained loading. *Constr. Build. Mater.* **2018**, *174*, 675–683. [CrossRef]
9. Li, C.; Yang, S.; Saafi, M. Numerical simulation of behavior of reinforced concrete structures considering corrosion effects on bonding. *ASCE J. Struct. Eng.* **2014**, *140*, 04014092. [CrossRef]
10. Manning, D.G. Corrosion performance of epoxy-coated reinforcing steel: North American experience. *Constr. Build. Mater.* **1996**, *10*, 349–365. [CrossRef]
11. Cairns, J.; Abdullah, R. Fundamental tests on the effect of an epoxy coating on bond strength. *ACI Mater. J.* **1994**, *91*, 331–338.
12. Tan, Z.; Hansson, C.M. Effect of surface condition on the initial corrosion of galvanized reinforcing steel embedded in concrete. *Corros. Sci.* **2008**, *50*, 2512–2522. [CrossRef]
13. Tang, F.; Chen, G.; Brow, R.K.; Volz, J.S.; Koenigstein, M.L. Corrosion resistance and mechanism of steel rebar coated with three types of enamel. *Corros. Sci.* **2012**, *59*, 157–168. [CrossRef]
14. Rossi, S.; Russo, F.; Calovi, M. Durability of vitreous enamel coatings and their resistance to abrasion, chemical, and corrosion: A review. *J. Coat. Technol. Res.* **2021**, *18*, 39–52. [CrossRef]
15. Rossi, S.; Zanella, C.; Sommerhuber, R. Influence of mill additives on vitreous enamel properties. *Mater. Des.* **2014**, *55*, 880–887. [CrossRef]
16. Izgagina, D.A.; Uglinskikh, M.Y.; Vlasova, S.G. Composition development and property study of alkali-resistance enamel for the protection of chemical apparatus. *Glass Ceram.* **2018**, *75*, 234–236. [CrossRef]
17. Jones, D.A. *Principles and Prevention of Corrosion*; Prentice Hall: Hoboken, NJ, USA, 1996.
18. Yang, X.; Jha, A.; Brydson, R.; Cochrane, R.C. An analysis of the microstructure and interfacial chemistry of steel-enamel interface. *Thin Solid Films* **2003**, *443*, 33–45. [CrossRef]
19. Wang, D. Effect of crystallization on the property of hard enamel coatings on steel substrate. *Appl. Surf. Sci.* **2009**, *255*, 4640–4645. [CrossRef]
20. Tang, F.; Chen, G.; Volz, J.S.; Brow, R.K.; Koenigstein, M. Microstructure and corrosion resistance of enamel coatings applied to smooth reinforcing steel. *Constr. Build. Mater.* **2012**, *35*, 376–384. [CrossRef]
21. Tang, F.; Chen, G.; Volz, J.S.; Brow, R.K.; Koenigstein, M.L. Cement-modified enamel coating for enhanced corrosion resistance of steel reinforcing bars. *Cem. Concr. Compos.* **2013**, *35*, 171–180. [CrossRef]
22. Tang, F.; Chen, G.; Brow, R.K. Chloride-induced corrosion mechanism and rate of enamel- and epoxy-coated deformed steel bars embedded in mortar. *Cem. Concr. Res.* **2016**, *82*, 58–73. [CrossRef]
23. Tang, F.; Cheng, X.; Chen, G.; Brow, R.K.; Volz, J.S.; Koenigstein, M.L. Electrochemical behavior of enamel-coated carbon steel in simulated concrete pore water solution with various chloride concentrations. *Electrochim. Acta* **2013**, *92*, 36–46. [CrossRef]
24. Yan, D.; Reis, S.; Tao, X.; Chen, G.; Brow, R.K.; Koenigstein, M. Effect of chemically reactive enamel coating on bonding strength at steel/mortar interface. *Constr. Build. Mater.* **2012**, *28*, 512–518. [CrossRef]
25. Moser, R.D.; Allison, P.G.; Williams, B.A.; Weiss Jr, C.A.; Diaz, A.J.; Gore, E.R.; Malone, P.G. Improvement in the geopolymer-to-steel bond using a reactive vitreous enamel coating. *Constr. Build. Mater.* **2013**, *49*, 62–69. [CrossRef]
26. Yang, F.; Yan, D.; Tang, F.; Chen, G.; Liu, Y.; Chen, S. Effect of sintering temperature on the microstructure, corrosion resistance and crack susceptibility of chemically reactive enamel (CRE) coating. *Constr. Build. Mater.* **2020**, *238*, 117720. [CrossRef]
27. Yan, D.; Xu, Z.; Qian, H.; Tang, F.; Liu, Y.; Huang, Z. Phase structure and corrosion resistance of multilayer low-temperature sintered chemically reactive enamel coatings. *ASCE J. Mater. Civ. Eng.* **2020**, *32*, 04020249. [CrossRef]
28. Yan, D.; Qian, H.; Huang, Z.; Tang, F.; Chen, G.; Deng, J.; Liu, Y. Study of lower temperature-sintered enamel coating on steel bars: Effect of coating cycles. *ASCE J. Mater. Civ. Eng.* **2020**, *32*, 04020262. [CrossRef]
29. Leechart, P.; Inthorn, D.; Thiravetyan, P. Effect of NaCl on antimony and phthalate compounds leached from PET bottles. *Water Supply* **2015**, *15*, 766–772. [CrossRef]
30. Cordoba-Torres, P. Relationship between constant-phase element (CPE) parameters and physical properties of films with a distributed resistivity. *Electrochim. Acta* **2017**, *225*, 592–604. [CrossRef]